INFECTION AND IMMUNITY, Aug. 1999, p. 4191–4200 Vol. 67, No. 8
0019-9567/99/$04.00+0

Plasma Membrane Expression of Heat Shock Protein 60 In Vivo in Response to Infection

CINDY BELLES, ALICIA KUHL,† RACHEL NOSHENY, AND SIMON R. CARDING*

Department of Clinical Studies, University of Pennsylvania, Philadelphia, Pennsylvania 19104-6010

Received 4 February 1999/Returned for modification 29 March 1999/Accepted 16 April 1999

Heat shock protein 60 (hsp60) is constitutively expressed in the mitochondria of eukaryotic cells. However, it has been identified in other subcellular compartments in several disease states and in transformed cells, and it is an immunogenic molecule in various infectious and autoimmune diseases. To better understand the factors that influence expression of hsp60 in normal cells in vivo, we analyzed its cellular and subcellular distribution in mice infected with the intracellular bacterium *Listeria monocytogenes*. Western blotting of subcellular fractionated spleen cells showed that although endogenous hsp60 was restricted to the mitochondria in noninfected animals, it was associated with the plasma membrane as a result of infection. The low levels of plasma membrane-associated hsp60 seen in the livers in noninfected animals subsequently increased during infection. Plasma membrane hsp60 expression did not correlate with bacterial growth, being most evident during or after bacterial clearance and persisting at 3 weeks postinfection. Using flow cytometry, we determined that Mac-1$^+$, T-cell receptor $\gamma\delta^+$, and B220$^+$ cells represented the major Hsp60$^+$ populations in spleens of infected mice. By contrast, B220$^+$ cells were the predominant hsp60$^+$ population in livers of infected mice. Of the immune cells analyzed, the kinetic profile of the $\gamma\delta$ T-cell response most closely matched that of hsp60 expression in both the spleen and liver. Collectively, these findings show that during infection hsp60 can be localized to the plasma membrane of viable cells, particularly antigen-presenting cells, providing a means by which hsp60-reactive lymphocytes seen in various infectious disease and autoimmune disorders may be generated and maintained.

Heat shock proteins (hsps) are highly conserved families of proteins which play essential roles in the folding, unfolding, and transport of proteins within both prokaryotic and eukaryotic cells (reviewed in reference 15). Although hsps are upregulated under a number of stress conditions, many are constitutively expressed in normal cells (28, 32, 33). The fact that deletion of hsp60 is lethal (14) emphasizes the essential role that this particular protein plays in protein assembly and cellular growth. hsp60 exists as a multimer composed of 7 or 14 hsp60 molecules in a toroid formation (30, 48) in the cytoplasm of prokaryotes or in the mitochondria of eukaryotes (4, 23). It has been estimated that at least half of the soluble proteins of *Escherichia coli* can form complexes with bacterial hsp60 (GroEL) while they are in unfolded or partially folded states (48), and hsp60 is utilized in the folding pathway for such enzymes as mouse dihydrofolate reductase (8, 30, 48) and ribulose-biphosphate carboxylase of *Rhodospirillum rubrum* (48).

hsp60 has been shown to be an immunodominant antigen of mycobacteria and other microorganisms (13, 26, 27). Mycobacterial hsp60 has been used as an adjuvant (39) and as a carrier molecule for conjugated vaccines (2, 38) and has been identified as an antigen for $\alpha\beta$ T cells in a rodent model of *Mycobacterium tuberculosis*-induced arthritis (47). Additionally, elevated anti-hsp60 antibodies have been detected in patients with juvenile chronic arthritis, diabetes mellitus, and cystic fibrosis (9), implying that hsp60 of either autologous or pathogenic origins may be present extracellularly in these diseases. The high degree of homology (>60%) between bacterial and mammalian forms of hsp60 has raised the possibility that hsp60 could be a potential antigen for autoimmune responses, and link microbial infection and autoimmunity (28). In addition to homology with microbial antigens, human hsp60 has sequence homology with a number of other autoantigens (26). Cross-reactivity between pathogenic hsp60s and other autologous proteins may, therefore, play a role in some autoimmune diseases.

Although the functional hsp60 complex does not normally appear outside the mitochondria in eukaryotes (23), several recent studies have identified hsp60 in other subcellular compartments under certain stress conditions or disease states. In studies using immunogold and electron microscopy, hsp60 has been identified in the secretory granules and plasma membranes of pancreatic cells of nonobese diabetic mice prior to the onset clinical disease (6). Mammalian hsp60 has been identified on the surface of cells within the lesions of brain tissue from patients with multiple sclerosis (MS) (44, 45), in sections of intestinal tissue from patients with inflammatory bowel disease (37), and in in vitro-propagated primary (24) as well as transformed (17) cell lines.

The significance of any extramitochondrial hsp60 expression by normal nontransformed cells in intact animals and the in vivo conditions under which this pattern of expression occurs are not known. The purpose of this study, therefore, was to investigate the expression of hsp60 in vivo in mice infected with the intracellular bacterium *Listeria monocytogenes* to determine whether hsp60 expression increases in various subcellular compartments during the course of infection and the host immune response, and to identify any hsp60 surface-positive (hsp60$^+$) cells.

MATERIALS AND METHODS

Animals. Female BALB/cByJ mice were obtained from the Jackson Laboratory (Bar Harbor, Maine) and were used between 8 and 12 weeks of age.

* Corresponding author. Mailing address: Department of Clinical Studies, University of Pennsylvania School of Veterinary Medicine, 3900 Delancy St., Philadelphia, PA 19104-6010. Phone: (215) 573-3022. Fax: (215) 573-6168. E-mail: carding@vet.upenn.edu.

† Present address: University of Colorado Health Science Center, Denver, CO 80262.

Antibodies and reagents. The hybridoma cell line 24G2, which secretes a monoclonal anti-mouse Fc receptor (FcR) antibody, was obtained from the American Tissue Culture Collection (Rockville, Md.), and intact antibody was isolated from culture supernatants by protein G affinity chromatography. The following antibodies were obtained from commercial sources. Anti-mouse T-cell receptor (TcR) αβ-fluorescein isothiocyanate (FITC) (clone H57-597), γδ TcR-FITC/phycoerythrin (PE) (GL3), Mac-1-FITC (M1/70-15), F480-PE (F4/80), B220-FITC/PE (RA3-6B2), GR1-FITC (RB6-8C5), CD3-FITC (500-A2), CD3-biotin/PE (CT-CD3), anti-mouse immunoglobulin G1 (IgG1)-biotin (LO-MG1), anti-mouse IgG1-horseradish peroxidase (HRP) (LO-MG1), anti-rabbit-FITC, strepavidin-allophycocyanin, and strepavidin-alkaline phosphatase (AP) were purchased from Caltag (San Francisco, Calif.); anti-mouse CD45.2-biotin (104) and Vδ4-FITC (GL2) were obtained from Pharmingen (San Diego, Calif.); strepavidin-FITC, -PE, and -Red670 were obtained from Life Technologies (Gaithersburg, Md.); the anti-hsp60 antibody LK2 was purchased from Stress-Gen (Vancouver, British Columbia, Canada). The anti-TcRVδ6.3 antibody 17C was generated in this laboratory (3). A rabbit anti-*Listeria* antiserum was kindly provided by Daniel Portnoy (University of California, Berkeley). A human antiserum reactive with subunits of the pyruvate dehydrogenase complex (PDC) from a patient with primary biliary cirrhosis was obtained from M. Eric Gershwin (University of California School of Medicine, Davis). Mouse and hamster IgG was purchased from Sigma (St. Louis, Mo.).

Preparation of *L. monocytogenes*. Stocks of *L. monocytogenes* wild-type strain 10403S were established as described previously (3). The LD_{50} (number of bacteria which caused lethality in 50% of adult BALB/c mice injected intravenously with *L. monocytogenes*) was empirically determined to be 3×10^4 CFU. Mice were injected via the tail vein with *L. monocytogenes* diluted in 100 μl of Ca^{2+}- and Mg^{2+}-free) phosphate-buffered saline (PBS). The number of *L. monocytogenes* in the spleen and liver was determined by weighing a portion of each tissue, homogenizing the tissue in a Dounce homogenizer, plating serial dilutions of the homogenate on Luria broth agarose plates, and determining the number of cfu after 16 to 24 h of incubation at 37°C. Lysates of *L. monocytogenes* for Western blotting experiments were prepared by lysozyme digestion and boiling as described elsewhere (41). Briefly, log-phase bacteria were pelleted, resuspended in 2 ml of lysozyme solution (2.5 mg/ml; Sigma), per ml, and incubated at 37°C for 90 min. The lysate was boiled for 5 min; 1 to 5 μg of protein was analyzed by sodium dodecyl sulfate-polyacrylamide gel electrophoresis (SDS-PAGE) to confirm cell lysis and protein integrity, aliquoted, and stored at −70°C until used.

Cytofluorometric analysis. Four-color fluorescence was used for the kinetic and phenotypic analysis of spleen and liver cells. Spleens and livers from infected mice were minced into cold (4°C) Hanks-buffered saline with 7% fetal calf serum and antibiotics (Hfa medium for spleen cells or into Hepatozyme medium (Life Technologies) containing 5% fetal calf serum and antibiotics for liver cells. Tissues were passed through 100-gauge nylon mesh to obtain a single-cell suspension. One hundred-microliter aliquots of 10^6 cells were added to individual wells of V-bottom 96-well microtiter plates. Staining of liver cells was performed in Hepatozyme medium to preserve the membrane integrity of hepatocytes. All antibody incubations were carried out on ice for 20 to 30 min each. Each sample was first incubated with the monoclonal anti-mouse FcR antibody 24G2 and mouse and/or hamster IgG to reduce nonspecific reactivity of antibodies with FcR^+ cells. After being washed with Hfa or Hepatozyme medium, cells were incubated with biotin-conjugated antibodies, washed, and then incubated with fluorochrome-conjugated strepavidin and fluorochrome-conjugated antibodies. For controls, duplicate cell samples were incubated with isotype-matched antibodies of irrelevant specificity. Stained cells were run on a FACScan (Becton Dickinson) and analyzed with CellQuest (Becton Dickinson) software.

Immunohistochemistry. A dual immunofluorescence-AP method was used to localize $hsp60^+$ and Mac-1^+ cells, or $hsp60^+$ and *L. monocytogenes*-infected cells, in the spleens of mice after infection with a sublethal dose (0.36 to 0.38 LD_{50}) of *L. monocytogenes*. Spleens were removed intact and snap-frozen in Tissue Tek (Miles Inc., Elkhart, Ind.)–2-methylbutane and stored at −80°C until sectioned. Frozen 7-μm sections were fixed in acetone and incubated with mouse IgG (50 μg/ml) diluted in Tris-buffered saline (TBS; 10 mM Tris–150 mM NaCl)–1% bovine serum albumin (TBS-BSA) to prevent nonspecific binding of antibodies. To visualize $hsp60^+$ and Mac-1^+ cells, sections were sequentially incubated with anti-Mac-1-biotin, strepavidin-AP, and anti-hsp60 (LK2)-FITC. To visualize $hsp60^+$ and *L. monocytogenes*-infected cells, sections were sequentially incubated with rabbit anti-*L. monocytogenes* antiserum, anti-hsp60 (LK2)-biotin, and anti-rabbit-FITC together with strepavidin-AP. Control, duplicate samples were incubated with isotype-matched antibodies or normal serum. The optimal concentration of each antibody was empirically determined in a series of preliminary experiments. Antibodies were diluted in TBS-BSA, and all incubations were performed in humidified chambers at 20°C for 30 min. In some instances AP staining was amplified by using a tertiary rat AP anti-AP antibody (Serotec/Harlan Bioproducts, Indianapolis, Ind.). AP activity was visualized by using the fluorescent Vector red substrate (Vector Laboratories, Burlingame, Calif.). Sections were counterstained with methyl green prior to mounting and photomicroscopy.

Subcellular fractionation. All procedures for fractionation were performed at 4°C. Cellular lysis and fractionation into nuclear, mitochondrial, cytoplasmic, plasma membrane, and secreted fractions were carried out by using a combined and modified version of the methods of Jett et al. (25), Balch and Rothman (1), Depierre and Dallner (10), and Hubbard (22). Briefly, four to seven mice per time point were sacrificed by cervical dislocation and immediately put on ice for dissection. Spleens and livers were removed, and a small portion of each taken to determine *L. monocytogenes* CFU. The remainder was weighed, minced in cold Dulbecco modified Eagle medium for spleens or cold Hepatozyme medium containing 0.05% (wt/vol) collagenase (Sigma) for livers, passed through 100-gauge nylon mesh to separate cells, and centrifuged at $200 \times g$ for 5 min. The supernatant was collected as the secreted protein fraction. The cell pellet was resuspended and washed in either Dulbecco modified Eagle medium or Hepatozyme medium, and the number and viability of cells were determined. Aliquots of cell suspensions were also tested for the presence of succinate reductase (SR) to determine whether mitochondria were intact. If SR activity was detected, then the cell samples were discarded. Three million cells were removed for fluorescence-activated cell sorting staining, and the remainder were lysed by the glycerol swell method (25). Glycerol in Hanks buffer (90%, vol/vol) was added to each solution in three equal increments 5 min apart for a final concentration of 30% glycerol. After the final addition of glycerol, cells were allowed to stand for 15 min for osmotic swelling.

Cells were then centrifuged at $1,200 \times g$ for 10 min, and the supernatant was taken as the glycerol fraction and tested for SR activity. Cells were then lysed by being quickly resuspending in hypotonic 0.25 M sucrose–10 mM Tris-HCl–1.5 mM $MgCl_2$ (0.25 M STM), incubated for 10 min with occasional vortexing, and then broken by 10 strokes in a Dounce homogenizer. A small volume of the lysate was then taken for marker enzyme assays, including SR assay (11, 36, 46). Cell lysis was also evaluated microscopically. The lysate was vortexed and overlaid onto 800 μl of 2.5 M STM (2.5 M sucrose, 10 mM Tris-HCl, 1.5 mM $MgCl_2$), which in turn was overlaid with 0.25 M STM prior to centrifugation at $100 \times g$ for 50 min at 4°C. The cytosol (upper portion) and nuclear (lower portion) fractions were removed and assayed for marker enzyme activity and protein content. The membrane fraction (interface) was broken by repeated pipetting and vortexing for 1 min prior to further fractionation on a discontinuous sucrose gradient into fractions of 200 μl each at densities of 1.300 (2.5 M STM) to 1.00 g/ml in increments of 0.015 g/ml (0.12 M STM) prepared in 5-ml polyvinyl centrifuge tubes. After centrifugation at $100 \times g$ for 75 min at 4°C, 13-drop fractions were collected by using a pump and capillary tubing until the first visible membrane interface was reached. Remaining fractions were removed by pipetting 250-μl increments from the gradient surface. Each fraction was then tested for marker enzyme activity. Membrane fractions containing high levels of mitochondrial marker enzyme (SR) activity and low levels of plasma membrane marker enzyme (alkaline phosphodiesterase I [APD]) activity were pooled as the mitochondrial fraction. Fractions with high levels of APD and low levels of SR were pooled and used as the plasma membrane fraction. All fractions were assayed for protein content by using the Bio-Rad (Hercules, Calif.) protein assay, diluted or concentrated if necessary, and then immediately analyzed by Western blotting. EL4 cell lysates were prepared by freezing intact cells in a dry ice-ethanol bath and transferring the cells to −20°C for 16 h, thawing them at room temperature, and boiling them for 5 min. The extent of cell lysis and protein integrity was evaluated by SDS-PAGE. Lysates were aliquoted and stored at −70°C until used.

Marker enzyme assays. Colorimetric assays were used to determine the level of enzyme activity in different subcellular fractions. Lactate dehydrogenase was used as the marker enzyme for the cytosol and was assayed as described previously (46). The assay for APD, used as the marker enzyme for the plasma membrane, was done with sodium thymidine 5′-monophosphate *p*-nitrophenyl ester (Sigma) as the substrate (36). The assay for SR, used as the marker enzyme for mitochondria, was done with 2-(*p*-indolphenyl)-3-(*p*-nitrophenyl-5-phenyl)tetrazolium (Sigma) as the substrate (36).

Western blotting. Fifteen micrograms of protein from each of the liver and spleen subcellular fractions or EL4 cell lysate and 20 μg of *L. monocytogenes* cellular protein were electrophoretically separated on 5-10-15% step gradient SDS-polyacrylamide gel G and transferred to Hybond-C nitrocellulose (Amersham, Arlington Heights, Ill.). Membrane blots were first blocked with TBS containing 5% dry milk powder for 60 min and then incubated with the mouse IgG1 anti-hsp60 antibody LK2 (80 μg/200 cm^2), diluted in TBS–5% milk for 60 min at 20°C. Blots were washed twice for 15 min in TBS with vigorous shaking and then incubated with 70 μg of anti-mouse IgG1-HRP in TBS–5% milk for 60 min with slow shaking. The blots were then washed briefly twice (15 min each) and once for 14 to 16 h before development using an enhanced chemiluminescence detection kit (Amersham). For reprobing of the blots with an anti-PDC antiserum, residual peroxidase activity was quenched, and the blots were incubated with the anti-PDC antiserum or normal human serum (1:4,000 dilution), washed, incubated with an HRP-conjugated anti-human Ig antibody (Caltag), and developed by chemiluminescence as described above.

RESULTS

Experimental approach. Female adult (6- to 8-week-old) BALB/c mice were infected intravenously (0.3 to 0.48 LD_{50}) with of *L. monocytogenes* 10403S, and the two major sites of infection, liver and spleen, were analyzed for expression of

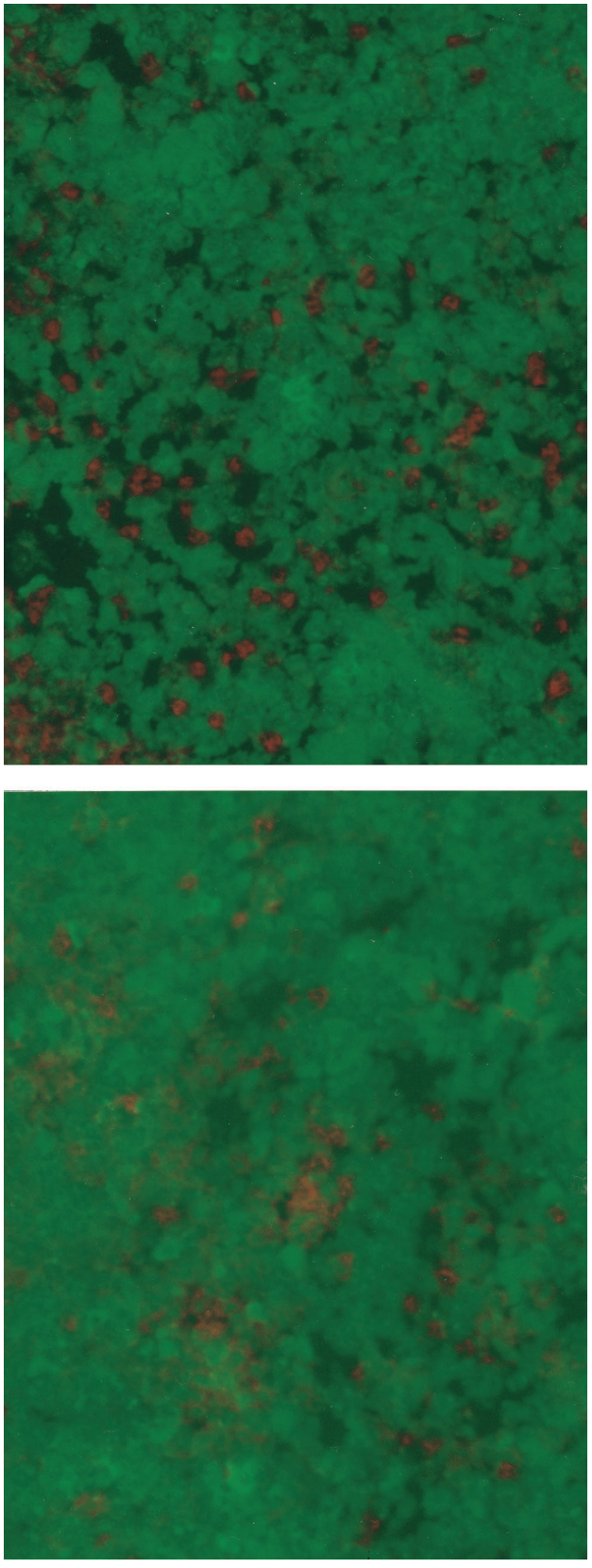

FIG. 1. Detection of hsp60 expression in spleens of *Listeria*-infected mice. Spleens from BALB/c mice 3 (top) and 6 (bottom) days after infection with *L. monocytogenes* (0.38 LD_{50}) were sectioned, fixed in acetone, and stained with antibodies specific for macrophages (Mac-1-biotin plus avidin-AP; red cells) and hsp60 (LK2-FITC; light green cells). The bottom photomicrograph shows that the majority of Mac-1^+ cells are also hsp60^+ and appear yellow-orange. The staining patterns shown are typical of those obtained in more than six independent experiments.

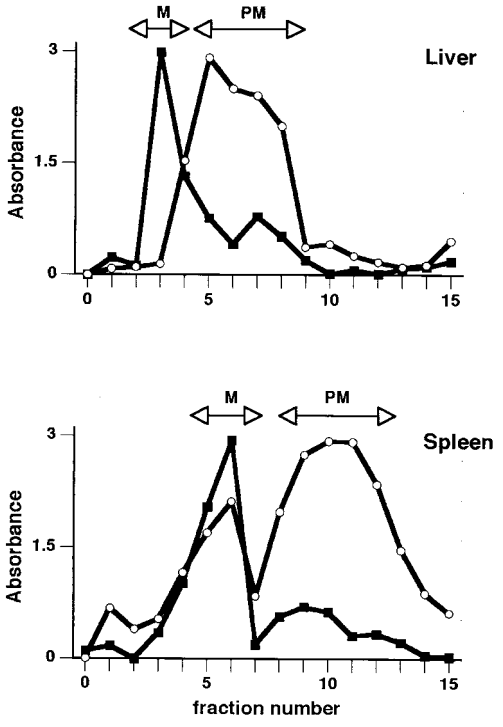

FIG. 2. Separation of mitochondria and plasma membrane of spleen and liver cells. Cells were fractionated, and individual fractions were tested for activity of marker enzymes for mitochondria (SR; ■) and plasma membrane APD; ○). Fractions containing highest levels of each enzyme (arrows labeled M for mitochondria and PM for plasma membrane) were combined and used as the final mitochondrial and plasma membrane fractions in Western blot experiments. Profiles are typical of those obtained in all experiments.

hsp60 by three independent methods. First, immunohistochemistry was used to identify hsp60 in situ in infected tissues. Second, subcellular fractionation and Western blotting were used to determine the subcellular distribution of hsp60 in spleen and liver cells of infected mice. Third, antibody staining and flow cytometry were used to identify and quantitate spleen and liver cells that might express surface hsp60 prior to and after infection.

Expression of hsp60 in situ in the spleen after infection with *L. monocytogenes*. Dual-label immunohistochemical analysis was used to localize hsp60 expression in situ in organ sections from infected mice. Tissues were snap-frozen, sectioned, and stained with antibodies for hsp60 (LK2-FITC) and Mac-1 (Mac-1–biotin plus avidin-AP) or with hsp60 (LK2-biotin plus avidin-AP) and a rabbit anti-*L. monocytogenes* antiserum (plus FITC-conjugated anti-rabbit Ig). Due to the inherently high autofluorescence and nonspecific staining in liver sections from infected mice, spleen sections were used for the majority of these experiments.

In sections of spleen from noninfected mice, it was not possible to detect any staining with the anti-hsp60 antibody LK2 above that of sections stained with control antibodies (data not shown). In infected animals, high levels of staining with LK2 were evident at day 3 in the spleen (Fig. 1), with the

TABLE 1. Determination of subcellular fraction purity by mitochondrial (SR) and plasma membrane (APD) marker enzyme activity

Day	Fraction	% of total enzyme activity (mean ± SD [n = 3])			
		Liver		Spleen	
		SR	APD	SR	APD
0	Nuclear	2.4 ± 1.9	2.8 ± 2.5	11.4 ± 1.0	4.2 ± 0.1
	Mitochondrial	92.5 ± 8.6	18.7 ± 15.6	66.9 ± 0.9	35.4 ± 3.8
	Cytosolic	0.1 ± 0.06	6.5 ± 5.2	11.4 ± 1.8	6.8 ± 5.7
	Plasma membrane	4.9 ± 6.6	76.2 ± 16.1	10.3 ± 1.7	53.6 ± 1.9
1	Nuclear	4.5 ± 3.1	2.8 ± 1.3	7.0 ± 2.1	24.0 ± 1.4
	Mitochondrial	77.8 ± 9.5	34.2 ± 8.8	74.0 ± 3.3	31.6 ± 2.8
	Cytosolic	1.1 ± 0.9	4.4 ± 0.9	6.4 ± 1.3	1.1 ± 0.5
	Plasma membrane	16.6 ± 11.4	58.6 ± 11.1	12.6 ± 0.1	43.3 ± 3.8
3	Nuclear	4.2 ± 6.3	2.1 ± 0.1	4.8 ± 2.3	9.1 ± 7.0
	Mitochondrial	78.4 ± 7.5	38.5 ± 1.7	79.8 ± 7.9	41.0 ± 4.8
	Cytosolic	3.9 ± 6.8	6.8 ± 0.8	5.3 ± 4.1	0.9 ± 0.6
	Plasma membrane	13.2 ± 6.5	52.7 ± 1.1	10.1 ± 1.4	49.0 ± 1.6
6	Nuclear	1.9 ± 3.6	1.7 ± 0.3	9.8 ± 0.2	13.2 ± 0.4
	Mitochondrial	93.1 ± 8.8	52.9 ± 7.4	66.2 ± 3.3	35.5 ± 11.6
	Cytosolic	2.0 ± 3.1	5.2 ± 0.2	13.7 ± 7.9	0.8 ± 0.1
	Plasma membrane	3.3 ± 2.1	40.5 ± 7.3	10.3 ± 4.4	50.5 ± 11.1
9	Nuclear	1.2 ± 2.3	1.9 ± 0.9	3.6 ± 1.8	13.0 ± 3.5
	Mitochondrial	89.2 ± 4.4	43.4 ± 8.0	76.1 ± 7.3	37.6 ± 1.2
	Cytosolic	1.7 ± 3.0	4.8 ± 3.1	9.7 ± 2.1	1.4 ± 0.6
	Plasma membrane	7.9 ± 1.1	50.7 ± 4.2	10.6 ± 3.3	48.0 ± 5.3
26	Nuclear	1.6 ± 2.7	1.0 ± 0.1	2.3 ± 0.4	12.0 ± 0.4
	Mitochondrial	81.9 ± 9.9	36.3 ± 2.8	83.3 ± 5.3	15.5 ± 0.1
	Cytosolic	2.5 ± 4.2	4.8 ± 3.8	2.4 ± 0.3	1.6 ± 0.1
	Plasma membrane	13.7 ± 2.5	57.9 ± 2.6	12.0 ± 4.4	70.9 ± 0.6

number of hsp60-stained cells increasing by 6 days postinfection. The halo-like pattern of staining and absence of any punctate cytoplasmic (mitochondrial) staining of intact cells in nonpermeabilized tissue sections was consistent with surface staining by the anti-hsp60 antibody (Fig. 1). Dual-staining experiments demonstrated that some hsp60$^+$ cells also expressed Mac-1, indicating that monocytes/macrophages were surface hsp60 positive after infection. Of note, the presence of orange-stained (Vector red plus FITC) cells in the spleen of mice at 6 days postinfection indicated that a large number of Mac-1$^+$ cells coexpressed hsp60.

Since bacterial numbers peak between 3 and 5 days postinjection in both liver and spleen (see Fig. 6F and 7F), the increase in level of hsp60 immunofluorescence staining seen at 6 days postinfection did not correlate with the level of *L. monocytogenes* found in each organ. Additional immunohistochemical staining experiments using a rabbit anti-*L. monocytogenes* antiserum in conjunction with the anti-hsp60 antibody demonstrated that the majority of *L. monocytogenes*-infected cells were not hsp60 surface positive (data not shown). This does not, however, exclude the possibility that at least some of the hsp60$^+$ macrophages that did not stain with the anti-*L. monocytogenes* antibody had previously taken up and destroyed the bacteria.

Increased hsp60 in mitochondrial and plasma membrane fractions of cells from livers and spleens of infected animals. Since the pattern of immunohistochemical staining was consistent with increased hsp60 in the plasma membrane of cells from infected tissues, we investigated the subcellular distribution of hsp60 in liver and spleen cells at various times after infection. A continuous subcellular fractionation protocol was developed to separate the nuclear, mitochondrial, cytosolic, and plasma membrane fractions of spleen and liver cells. Equivalent amounts of total protein of each fraction were then electrophoretically separated, transferred to nitrocellulose, and probed for hsp60 by Western blotting. Since our main interest was in evaluating the amount of hsp60 associated with the plasma membrane and to minimize the possibility that hsp60 from mitochondria could contaminate other fractions, the subcellular fractionation protocol was developed to optimize the purity of the plasma membrane fraction.

Figure 2 depicts results that are typical of the final step in separating the mitochondria from the plasma membrane and the assaying of individual fractions from the discontinuous density gradient for the mitochondrial enzyme marker SR and the plasma membrane enzyme marker APD. Fractions showing peak activity and minimal cross-contamination were collected, pooled, and used as the mitochondrial and plasma membrane fractions in subsequent Western blotting experiments. In addition, nuclear and cytosolic fractions were also tested for APD and SR activity to determine fraction purity (Table 1). In the liver, the level of contamination of the plasma membrane fractions with SR ranged from 3.3% ± 2.1% of the total activity detected in all of the subcellular fractions on day 6 to 16.6% ± 11.4% on day 1. The level of SR activity present in the plasma membrane fractions of the spleen ranged from 10.1% ± 1.4% on day 3 to 12.6% ± 0.1% on day 1. As expected, the highest levels of SR activity were found in the mitochondrial fractions of both the liver (78 to 93%) and spleen (66 to 83%).

Equivalent amounts of total protein from each of the four subcellular fractions of spleen and liver cells from mice at

TABLE 2. Subcellular distribution of hsp60 in spleen and liver fractions of *Listeria*-infected mice, determined by densitometry readings

Fraction	% of total hsp60 expression (mean ± SD [n = 3])					
	Day 0	Day 1	Day 3	Day 6	Day 9	Day 26
Liver						
Nuclear	2.1 ± 4.0	22.0 ± 4.7	11.5 ± 5.9	13.1 ± 7.5	18.4 ± 7.5	14.0 ± 1.4
Mitochondrial	47.2 ± 13.9	37.0 ± 19.0	37.2 ± 12.4	34.1 ± 6.9	40.3 ± 21.4	10.4 ± 0.1
Cytoplasmic	24.1 ± 9.6	26.7 ± 19.8	39.4 ± 3.8	21.4 ± 5.3	16.9 ± 5.0	13.1 ± 6.3
PM[a]	26.7 ± 9.8	14.3 ± 5.5	11.8 ± 4.4	31.5 ± 3.4	24.4 ± 18.4	62.5 ± 7.9
PM as % of mitochondria	55.6	38.6	31.7	92.4	60.5	600.9
Spleen						
Nuclear	6.2 ± 3.4	2.0 ± 2.0	15.2 ± 14.3	18.3 ± 11.9	9.2 ± 8.4	0.1 ± 0.5
Mitochondrial	82.5 ± 0.6	94.3 ± 21.3	67.2 ± 15.9	46.4 ± 5.1	66.7 ± 12.2	65.1 ± 0.2
Cytoplasmic	0.7 ± 2.8	2.1 ± 4.0	2.1 ± 2.7	15.4 ± 2.8	2.6 ± 0.1	0.1 ± 4.9
PM	10.5 ± 0.1	1.5 ± 2.9	15.5 ± 1.3	19.9 ± 8.0	21.5 ± 10.9	34.7 ± 4.1
PM as % of mitochondria	12.7	1.6	23.1	42.9	32.2	53.1

[a] PM, plasma membrane.

various times after infection were analyzed by Western blotting for expression of hsp60, using antibody LK2 and chemiluminescence to detect bound antibody. Scanning densitometry of developed blots was used to determine the relative amounts and distribution of hsp60 in the fractions of each sample (Table 2). As controls, total cell lysates from *L. monocytogenes* and EL4, a mouse lymphoma cell line, were included on each gel (Fig. 3). Since the LK2 antibody reacted with EL4 but not *L. monocytogenes*, the hsp60 identified on these blots was autologous murine hsp60.

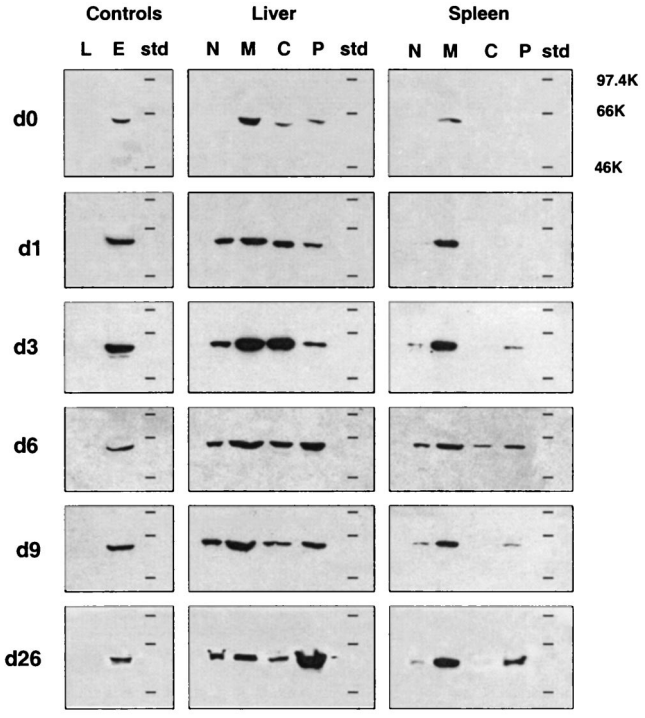

FIG. 3. Subcellular distribution of hsp60 in vivo during infection. Spleen and liver cells from mice at various times (days [d]) after infection with *L. monocytogenes* (0.34 LD_{50}) were fractionated, and 15 μg of protein from the nuclear (N), mitochondrial (M), cytoplasm (C), and plasma membrane (P) fractions were analyzed for hsp60 expression by Western blotting. Molecular weight markers (std) and total cell lysates of *L. monocytogenes* (20 μg; L) and EL4 (15 μg; E) were included on each gel. The results shown are representative of those obtained in three independent experiments. The horizontal lines on each blot represent positions of molecular weight standards (97.4, 66, and 46 kDa).

Endogenous hsp60 expression in the various subcellular compartments changed during the course of infection (Fig. 3 and Table 2) and remained high as long as 3 weeks after infection. In the liver, hsp60 expression in naive animals (day 0) was mainly restricted to the mitochondrial fraction, although the cytoplasmic and plasma membrane fractions contained low levels of hsp60. During the course of infection, the level of hsp60 in the plasma membrane fractions increased until day 6 and then declined by day 9. Levels of mitochondrial hsp60 also increased, peaking on day 3. A large increase in plasma membrane hsp60 was seen on day 26, more than 2 weeks after resolution of the infection, and was over sixfold higher than the level of hsp60 seen in the mitochondria at this time (Table 2).

In spleens of naive mice, hsp60 was, as expected, localized to the mitochondria, no hsp60 was detected in the other cellular fractions, including the plasma membrane. Three days after infection, hsp60 was detected in the plasma membrane fractions, with relatively higher levels seen on day 6 (Fig. 3). Subsequently, the plasma membrane levels decreased at day 9 and then increased again at 3 weeks postinfection, similar to the pattern seen in the liver. Consistent with the results of the immunohistochemical studies, the profile of hsp60 expression in the plasma membrane fractions did not coincide with that of bacterial CFU in either organ (see Fig. 6F and 7F).

The purity of the plasma membrane fractions (Table 1) and level of hsp60 expression in each of the subcellular fractions (Table 2) strongly suggest that the plasma membrane-associated hsp60 seen in organs from infected mice is unlikely to be attributable to contamination by mitochondrial proteins. If the plasma membrane-associated hsp60 was due to mitochondria leakage or damage and cross-contamination, the plasma membrane fractions should contain similar amounts of other mitochondrial proteins, such as SR. This is not the case. For example, in liver cell samples from day 6, at which high levels of hsp60 are detected in plasma membrane fractions, approximately one-third of the total hsp60 present is in the plasma membrane fraction, whereas only 3% of the total mitochondria SR activity is found in this fraction. Similarly, the day 6 plasma membrane fraction in the spleen accounts for approximately 20% of the total hsp60 but only 10% of the SR activity. Samples from day 26 postinfection emphasize this point further, with 63% of the total hsp60 expression and 14% SR activity

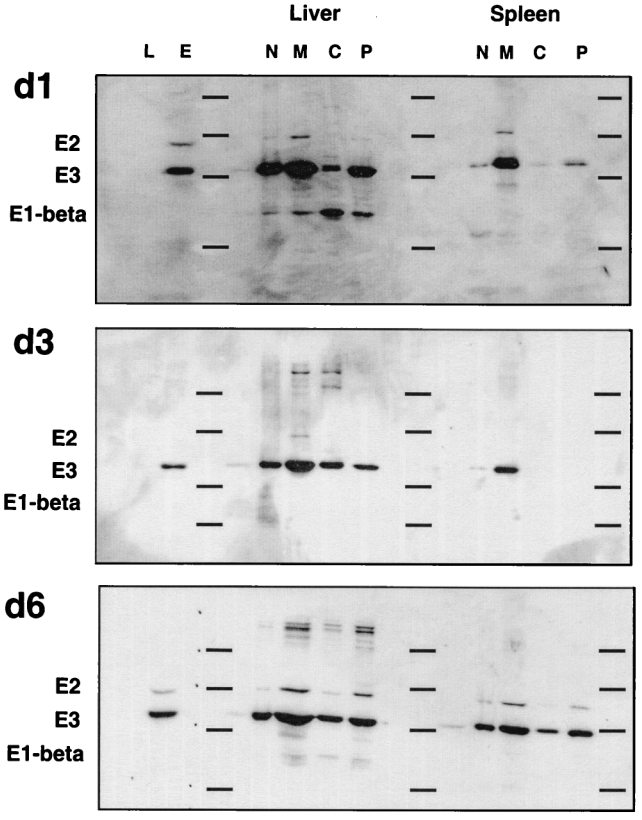

FIG. 4. Subcellular distribution of the PDC in spleens and livers of *Listeria*-infected mice. Western blots originally probed with anti-hsp60 antibody (Fig. 3) were stripped and reprobed with an antiserum from a patient with primary biliary cirrhosis containing high-titer antibodies to PDC. Bound antibody was visualized by chemiluminescence as described in the legend to Fig. 3. The subunits of PDC present in the samples are indicated on the left. The horizontal lines on each blot represent positions of molecular weight standards (97.4, 66, 46, and 30 kDa). d1, d3, and d6, 1, 3, and 6 days postinfection.

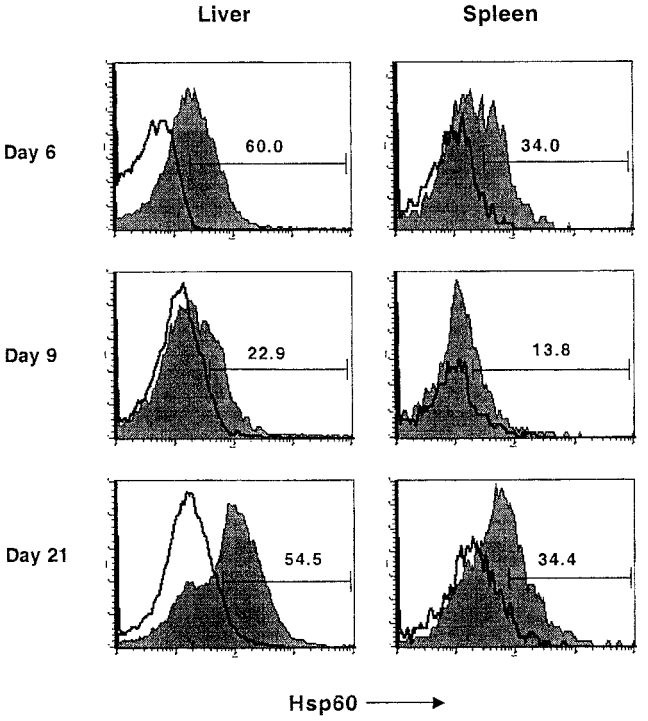

FIG. 5. Increased hsp60 expression on macrophages in livers and spleens of infected mice. Spleen and liver cells obtained from mice at various times after infection were analyzed by flow cytometry. hsp60 expression by monocytes/macrophages was determined by gating on Mac-1^+ cells and analyzing for hsp60 expression. The filled and open plots show profiles of staining obtained with anti-hsp60 (filled profiles) and an isotype-matched antibody, respectively; numbers represent percentages of Mac-1^+ cells which are hsp60^+.

present in the liver plasma membrane fraction, while 35% of the total hsp60 and 12% of the SR are present in the plasma membrane fraction of the spleen. The subcellular redistribution and localization to the plasma membrane of mitochondrial proteins was, however, not unique to hsp60.

Reprobing of the Western blots analyzed for hsp60 with an antiserum containing high-titer antibodies to the mitochondrial PDC showed that subunits of this complex, particularly E3, were also associated with the plasma membrane fractions of spleen and liver cells (Fig. 4). Importantly, however, the profiles of PDC and hsp60 plasma membrane expression were nonoverlapping. Plasma membrane-associated hsp60 was detected in the absence of PDC (compare data for day 3 in Fig. 3 and 4) and vice versa (day 1 in Fig. 3 and 4). Plasma membrane expression of PDC was not consistent, and E3 expression in the plasma membrane was sometimes higher than in mitochondrial fractions, which argues against the redistribution of PDC (or hsp60) being attributable to contamination by mitochondrial proteins during the fractionation procedure.

Identification of cells expressing surface hsp60. Four-color flow cytometric analysis was used to identify and quantitate cells of different lineages that express surface hsp60 before and at various times after infection. Light scatter properties and/or vital dye stains were used to exclude apoptotic and dead cells from this analysis. The number of granulocytes (GR1^+), monocytes/macrophages (Mac-1^+), B cells (B220^+), $\alpha\beta$ T cells ($\alpha\beta$TcR$^+$), and $\gamma\delta$ T cells ($\gamma\delta$TcR$^+$) was determined from the frequency of stained cells and the total number of viable cells recovered from each tissue. Isotype-matched antibodies of irrelevant specificity were used to determine levels of background staining.

Representative anti-hsp60 antibody staining profiles for Mac-1^+ spleen and liver cells are shown in Fig. 5. Consistent with the results of the subcellular fractionation and Western blotting experiments, flow cytometric analysis confirmed plasma membrane expression of hsp60. The profiles of hsp60 expression in both the liver and spleen as determined by these two methods were also comparable. In the liver, the total number of hsp60^+ cells increased up to day 6 postinfection, after which it decreased at day 9 and then increased again at day 21 (Fig. 6F). As was seen in the immunohistochemistry and subcellular fractionation experiments, hsp60 expression did not correlate with bacterial numbers, which peaked on day 3 and were no longer detected by day 9 postinfection (Fig. 6).

Macrophages, B cells, and $\gamma\delta$ T cells were the major hsp60-expressing cells in the liver. On day 6, the first peak of hsp60^+ cells, macrophages (31%), and $\gamma\delta$ T cells (27%) made up the majority of the hsp60^+ cells (Table 3). By day 21 postinfection, corresponding to a second peak in hsp60^+ cells, the majority of hsp60^+ cells were B220^+ (31%) or $\gamma\delta$ T cells (35%). Of note, the kinetic profile of $\gamma\delta$ T cells most closely matched that of hsp60^+ cells, with the number of $\gamma\delta$ T cells peaking on days 6 and 21 postinfection coincident with peaks of hsp60^+ cells (Fig. 6). As seen previously (3), V$\delta4^+$ and V$\delta6.3^+$ cells dominated the $\gamma\delta$ T-cell response to *L. monocytogenes* infection (data not shown). The largest number of $\gamma\delta$ T cells was seen at

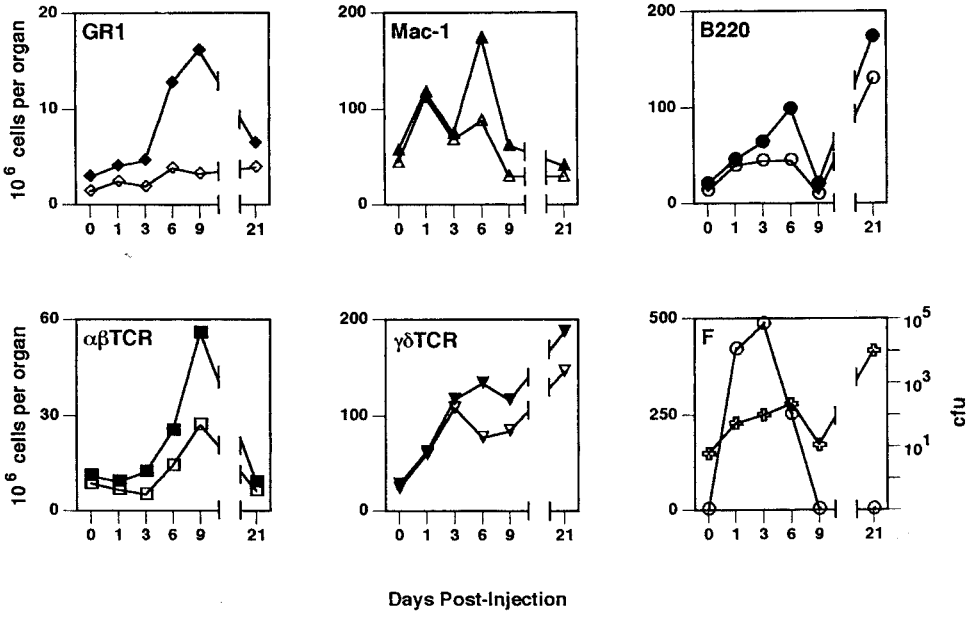

FIG. 6. Kinetic profiles of cellular response, hsp60 expression, and bacteria in the liver. Before and at various times after infection with *L. monocytogenes* (0.30 LD_{50}), the numbers of granulocytes (GR1), monocytes/macrophages (Mac-1), B cells (B220), αβ T cells (αβTcR) and γδ T cells (γδTcR) present in the liver were determined from total cell counts, and the proportion of cells reactive with lineage-specific antibodies as determined by flow cytometry. Closed symbols, total cell numbers; open symbols, numbers of $hsp60^+$ cells of each cell subtype. Panel F shows the bacterial CFU (○) and total number of surface $hsp60^+$ cells (✠). All values are means from four animals. Standard deviations were <20% in all cases and for the sake of clarity are not shown.

3 days postinfection and 21 days postinfection, at which time the majority were also $hsp60^+$ (Fig. 6). Also of note was the large number of $B220^+$ cells present in the liver at 21 days postinfection. By contrast, $GR1^+$ and $\alpha\beta TcR^+$ cells reached maximal numbers on day 9. With the exception of $\alpha\beta TcR^+$ cells at 9 days postinfection, αβ T cells and granulocytes comprised less than 6% of $hsp60^+$ cells throughout infection (Table 3).

As seen in the liver, the kinetic profile of hsp60 cell surface expression in the spleen did not correlate with that of bacterial numbers (Fig. 7F). Although the number of $GR1^+$, $\alpha\beta TcR^+$, and $\gamma\delta TcR^+$ cells showed similar kinetic profiles in the spleen as in the liver, the profile of macrophages and B cells were distinct (Fig. 7). In contrast to the liver, $B220^+$ cells represented the largest population of $hsp60^+$ cells in the spleen at all of the time points analyzed (Table 3). Similar to the liver, the kinetic profile of total γδ T cells most closely matched that of $hsp60^+$ cells (Fig. 7), and the response was dominated by $V\delta4^+$ or $V\delta6.3^+$ cells (data not shown). In addition, γδ T cells also made up a significant proportion (15 to 30%) of $hsp60^+$ cells, particularly after 3 days postinfection, similar to that seen in the liver (Table 3).

In summary, the profile of hsp60 expression in the livers and spleens of infected mice is concordant with that obtained by subcellular fractionation and Western blotting. The compositions of $hsp60^+$ cells are, however, different in these tissues, although antigen-presenting (APCs) cells are the predominant $hsp60^+$ population in the liver (macrophages) and spleen (B cells). Finally, whereas the kinetic profile of plasma membrane-associated hsp60 expression does not overlap with bacterial numbers, it does parallel the kinetics of γδ T-cell involvement in both liver and spleen.

DISCUSSION

The results described in this study demonstrate that the cellular and subcellular distribution of hsp60 in cells of the liver and the spleen changes in response to *L. monocytogenes* infection. Using three independent experimental approaches, we have shown that although hsp60 is not found on cell surfaces in healthy noninfected animals, *L. monocytogenes* infection results in expression of hsp60 on the plasma membrane of viable intact cells in the liver and spleen. In particular, APCs such as B cells and macrophages are surface $hsp60^+$. In addi-

TABLE 3. Distribution of $hsp60^+$ cells in the liver and spleen, determined by flow cytometric analysis

Day	% of total $hsp60^+$ cells (mean ± SD [n = 4])										
	Liver						Spleen				
	$B220^+$	$Mac\text{-}1^+$	$\alpha\beta TCR^+$	$\gamma\delta TCR^+$	$GR1^+$	Other	$B220^+$	$Mac\text{-}1^+$	$\alpha\beta TCR^+$	$\gamma\delta TCR^+$	$GR1^+$
0	8.8 ± 2.8	29.7 ± 11.6	5.8 ± 2.4	15.4 ± 7.3	0.9 ± 0.8	39.3 ± 11.0	65.6 ± 21.3	15.4 ± 5.2	4.1 ± 3.7	15.0 ± 7.4	0.0 ± 0.0
1	17.0 ± 5.6	49.0 ± 14.9	2.9 ± 1.7	25.9 ± 13.6	1.1 ± 0.3	4.2 ± 2.7	57.7 ± 16.5	20.4 ± 10.6	3.3 ± 3.0	14.6 ± 5.9	4.5 ± 1.4
3	7.6 ± 3.3	27.3 ± 9.3	2.0 ± 1.4	43.1 ± 15.3	0.8 ± 0.4	9.2 ± 3.0	48.8 ± 22.9	22.5 ± 9.4	1.1 ± 1.0	24.9 ± 8.3	2.7 ± 1.2
6	15.9 ± 2.8	31.5 ± 18.8	5.1 ± 2.8	27.5 ± 4.5	1.4 ± 0.7	18.5 ± 2.8	45.8 ± 7.0	13.1 ± 5.2	9.0 ± 3.2	30.1 ± 4.3	1.5 ± 0.4
9	5.5 ± 3.2	17.1 ± 7.1	15.8 ± 6.2	48.7 ± 17.1	1.9 ± 1.1	11.1 ± 3.2	58.7 ± 21.6	9.9 ± 1.8	8.3 ± 3.5	17.0 ± 1.3	3.2 ± 1.6
21	31.1 ± 4.3	7.1 ± 4.7	1.5 ± 0.8	35.0 ± 12.8	0.9 ± 0.8	24.4 ± 6.4	54.5 ± 9.7	11.1 ± 1.9	6.6 ± 2.4	23.7 ± 1.4	0.5 ± 0.4

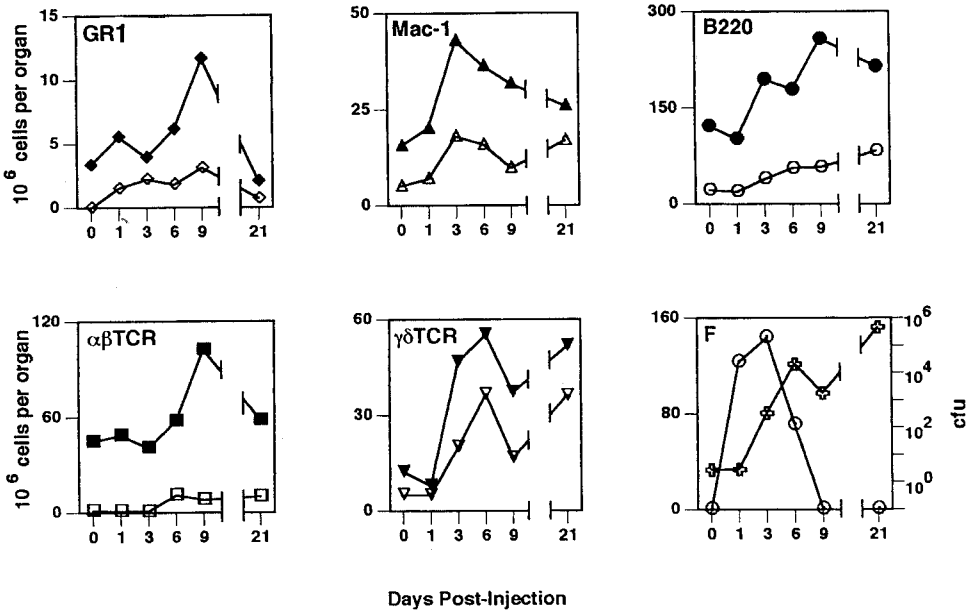

FIG. 7. Kinetic profiles of the cellular response, hsp60 expression, and bacteria in the spleen. Spleen cells were analyzed and the different populations were enumerated as described in the legend to Fig. 6. Closed symbols, total cell numbers; open symbols, numbers of hsp60$^+$ cells of each cell subtype. Panel F shows bacterial CFU (○) and total number of surface hsp60$^+$ cells (⊕). All values are means from four animals. Standard deviations were <20% in all cases and for the sake of clarity are not shown.

tion, our results demonstrate that surface hsp60 expression does not correlate with the kinetics of bacterial growth. Surprisingly, elevated levels of hsp60 are still present 2 weeks after resolution of the disease.

Although we know neither how the subcellular distribution of hsp60 is regulated nor the biological significance of plasma membrane-associated hsp60, there are several possible explanations. Increased hsp60 on cell surfaces could simply be an indicator of cellular stress, possibly produced directly by infection or indirectly by cytokines and fever. Production and repair of proteins increase during stress and infection, and hsp60 is necessary to these processes (15). hsps also have long half-lives, and so it is possible that hsp60 is transported to the cell surface as a way to eliminate excess hsp. If hsp60 is expelled from the cell, hsp60-derived peptides would then become displayed on the surfaces of professional APCs. Considering that hsp60 is a major immunogen of many bacterial pathogens (26, 27) and that there is a high level of homology between bacterial and mammalian hsp60 (28), this process could sustain activated T cells primed to respond to a number of pathogens, as well as contribute to autoimmune disease.

Another possibility is that surface hsp60 acts as a signal of stressed, activated, or damaged cells, targeting them for clearance by cytotoxic cells or macrophages as part of the tissue repair process. In our infectious disease model hsp60 could be expressed on preapoptotic or apoptotic cells. Increased levels of hsp60 expression have been detected on membranes of cells induced to undergo apoptosis by treatment with dexamethasone (40) and also in apoptotic cells isolated directly from AIDS patients (40). T cells undergoing antigen-triggered apoptosis in vivo disappear from the lymph nodes and spleen and accumulate in the liver, where they undergo apoptosis and are cleared from the body (20, 21). Livers of *L. monocytogenes*-infected mice contains a large population of small viable cells (as indicated by low forward scatter) that are highly granular (high side scatter) and increase in number up to day 21, at which time 85% are B220$^+$, 15% are γδTcR$^+$, and 95 to 98% are hsp60$^+$ (2a). These cells may have already encountered antigen and be undergoing activation-induced apoptosis, accumulating in the liver awaiting clearance.

Although examples of secretion of hsp60 have been described for parasites (13), we have been unable to detect secretion of hsp60 by spleen or liver cells in vivo during listeriosis. We have also been unable to detect hsp60 in the supernatants of cultured hybridoma lines expressing hsp60 on their cell surfaces (2a). It is possible that autologous hsp60 exists at the cell surface as an intact toroid form rather than as peptide fragments associated with major histocompatibility complex molecules. Since the hsp60 toroid form often contains other proteins, and the hsp60 complex can retain denatured proteins that it cannot fold (7, 15, 16), one possibility is that under conditions of hyperactivation or stress, hsp60 chaperones (abnormal) proteins to the cell surface for their elimination. The observation that hsp60 in the plasma membrane of the human T-cell leukemic cell line CEM-SS attaches to the H2B histone protein and is released as a result of protein kinase A-catalyzed phosphorylation (29) is consistent with the ability of hsp60 to expel proteins from the plasma membrane under certain conditions. Plasma membrane hsp60 might be recognized by T cells as a complex containing proteins the cell is trying to expel. It is also possible that the structural changes of the hsp60 toroid form that occur when it complexes with other cellular proteins (43) reveal conformational determinants recognized by immune cells.

It is interesting that of the cell populations analyzed during *L. monocytogenes* infection, the kinetics of the γδ T-cell response most closely matches that of hsp60 expression. Several groups have postulated that hsp60 is a ligand for γδ T cells (5, 35). γδ T cells and hsp60$^+$ oligodendrocytes have been colocalized in sections of demyelinated brain tissue from patients with MS (44, 45), and γδ T cells have been shown in vitro to kill oligodendrocytes isolated from MS patients (12). Also, hsp60-

reactive γδ T cells have been isolated from the synovial fluid of patients with rheumatoid arthritis (19), and synovial γδ T cells from patients with Lyme arthritis can induce apoptosis of synovial $CD4^+$ αβ T lymphocytes via Fas-Fas ligand interactions (49). $hsp60^+$ cells (37) and large numbers of mycobacterial hsp60-reactive γδ T cells (31) are found in the intestinal lesions of patients with inflammatory bowel disease. Additionally, populations of peritoneal exudate cells from *L. monocytogenes*-infected mice that were enriched for γδ T cells have been shown to proliferate and release gamma interferon after culture with recombinant mycobacterial hsp60 (18).

We have previously shown that a large proportion of γδ T cells that accumulate in both livers and spleens of *L. monocytogenes*-infected mice express a TcR encoded by either Vδ6 or Vδ4 (3), both of which have been previously shown to correlate with hsp60 reactivity (34). The observation that $V\delta6^+$ γδ T cells from *L. monocytogenes*-infected mice reacts with plasma membrane preparations of *L. monocytogenes*-elicited, $hsp60^+$ peritoneal exudate cells (36a) suggests that γδ T cells may indeed respond to and recognize hsp60 expressed in the plasma membrane of cells in response to infection. If these γδ T cells react with hsp60 on the cell surface, they may recognize the hsp60 alone or complexed with an interior protein in a manner similar to major histocompatibility complex presentation of peptides. Although liver and spleen γδ T cells have limited γ- and δ-chain pairing, these receptors, particularly the δ chain, have diverse junctional sequences (34, 42). These cells may, therefore, recognize the hsp60 portion of such a complex with the γ/δ constant regions and any variation of interior proteins with junctional regions. The molecular nature of γδ T cell-hsp60 interactions is currently being investigated in our laboratory.

ACKNOWLEDGMENTS

This work was supported by Public Health Service grants AI-31972, AI-45993, and HL-51749 from the National Institutes of Health and by a grant from the University of Pennsylvania Research Foundation.

REFERENCES

1. **Balch, W. E., and J. E. Rothman.** 1985. Characterization of protein transport between successive compartments of the Golgi apparatus: asymmetric properties of donor and acceptor activities in a cell-free system. Arch. Biochem. Biophys. **240:**413–425.
2. **Barrios, C., A. R. Lussow, J. van Embden, R. van der Zee, R. Rappuoli, P. Constantino, J. A. Louis, P.-H. Lambert, and G. Del Giudice.** 1992. Mycobacterial heat-shock proteins as carrier molecules II: the use of the 70-kDa mycobacterial heat-shock protein as carrier for conjugated vaccines can circumvent the need for adjuvants and Bacillus Calmette Guerin priming. Eur. J. Immunol. **22:**1365–1372.

2a. **Belles, C., and S. R. Carding.** Unpublished observations.

3. **Belles, C., A. L. Kuhl, A. J. Donoghue, Y. Sano, R. L. O'Brien, W. Born, K. Bottomly, and S. R. Carding.** 1996. Bias in the γδ cell response to Listeria monocytogenes: $V\delta6.3^+$ cells are a major component of the γδ T cell response to Listeria monocytogenes. J. Immunol. **156:**4280–4289.
4. **Boog, C. J. P., E. R. de Graeff-Meeder, M. A. Lucassen, R. van der Zee, M. M. Voorhorst-Ogink, J. S. van Kooten, H. J. Geuze, and W. van Eden.** 1992. Two monoclonal antibodies generated against human HSP60 show reactivity with synovial membranes of patients with juvenile chronic arthritis. J. Exp. Med. **175:**1805–1810.
5. **Born, W. K., R. L. O'Brien, and R. L. Modlin.** 1991. Antigen specificity of γδ T lymphocytes. FASEB J. **5:**2699–2705.
6. **Brudzynski, K., V. Martinez, and R. S. Gupta.** 1992. Immunocytochemical localization of heat-shock protein 60-related protein in beta-cell secretory granules and its altered distribution in non-obese diabetic mice. Diabetologia **35:**316–324.
7. **Burston, S. G., J. S. Weissman, G. W. Farr, W. A. Fenton, and A. L. Horwich.** 1996. Release of both native and non-native proteins from a cis-only GroEL ternary complex. Nature **383:**96–99.
8. **Clark, A. C., E. Hugo, and C. Frieden.** 1996. Determination of regions in the dihydrofolate reductase structure that interact with the molecular chaperonin GroEL. Biochemistry **35:**5893–5901.
9. **de Graeff-Meeder, E. R., G. T. Rijkers, M. M. Voorhorst-Ogink, W. Kuis, R. van der Zee, W. van Eden, and B. J. M. Zegers.** 1993. Antibodies to human Hsp60 in patients with juvenile chronic arthritis, diabetes mellitus, and cystic fibrosis. Pediatr. Res. **34:**424–428.
10. **Depierre, J. W., and G. Dallner.** 1975. Structural aspects of the membrane of the endoplasmic reticulum. Biochim. Biophys. Acta **415:**411–472.
11. **Dignam, J. D.** 1990. Preparation of extracts from higher eukaryotes. Methods Enzymol. **182:**194–203.
12. **D'Souza, S. D., J. P. Antel, and M. S. Freedman.** 1994. Cytokine induction of heat shock protein expression in human oligodendrocytes: an interleukin-1 mediated mechanism. J. Neuroimmunol. **50:**17–24.
13. **Ernani, F. P., and J. M. Teale.** 1993. Release of stress proteins from *Mesocestoides corti* is a brefeldin A-inhibitable process: evidence for active export of stress proteins. Infect. Immun. **61:**2596–2601.
14. **Fayet, O., T. Ziegelhoffer, and C. Georgopoulos.** 1989. The *groES* and *groEL* heat shock gene products of *Escherichia coli* are essential for bacterial growth at all temperatures. J. Bacteriol. **171:**1379–1385.
15. **Fenton, W. A., and A. L. Horwich.** 1997. GroEL-mediated protein folding. Protein Sci. **6:**743–760.
16. **Fenton, W. A., Y. Kashl, K. Furtak, and A. L. Horwich.** 1994. Residues in chaperonin GroEL required for polypeptide binding and release. Nature **371:**614–619.
17. **Fisch, P., M. Malkovsky, S. Kovats, E. Strum, E. Braakman, and P. Sondel.** 1990. Recognition by human Vγ9/Vδ2 T cells of a GroEL homolog on Daudi Burkitt's lymphoma cells. Science **250:**1269–1273.
18. **Hiromatsu, K., Y. Yoshikai, G. Matsuzaki, S. Ohga, K. Muramori, K. Matsumoto, J. A. Bluestone, K. Nomoto.** 1992. A protective role of γδ T cells in primary infection with *Listeria monocytogenes* in mice. J. Exp. Med. **175:**49–56.
19. **Holoshitz, J., F. Koning, J. E. Coligan, J. de Bruyn, and S. Strober.** 1989. Isolation of $CD4^-CD8^-$ mycobacteria-reactive T lymphocyte clones from rheumatoid arthritis synovial fluid. Nature **339:**226–229.
20. **Huang, L., G. Soldevilla, M. Leeker, and R. Flavell.** 1994. The liver eliminates T cells undergoing antigen-triggered apoptosis in vivo. Immunity **1:**741–749.
21. **Huang, L., K. Sye, and I. N. Crispe.** 1994. Proliferation and apoptosis of $B220+CD4-\ CD8-TCR\alpha\beta^{intermediate}$ T cells in the liver of normal adult mice: implication for lpr pathogenesis. Int. Immunol. **6:**533–540.
22. **Hubbard, A. L., D. A. Wall, and A. Ma.** 1983. Isolation of rat hepatocyte plasma membranes. I. Presence of the three major domains. J. Cell Biol. **96:**217–229.
23. **Itoh, H., R. Kobayashi, H. Wakui, A. Komatsuda, H. Ohtani, A. B. Miura, M. Otaka, O. Masamune, H. Andoh, K. Koyama, Y. Sato, and Y. Tashima.** 1995. Mammalian 60-kDa stress protein (chaperonin homolog): identification, biochemical properties, and localization. J. Biol. Chem. **270:**13429–13435.
24. **Jarjour, W., L. A. Mizzen, W. J. Welch, S. Denning, M. Shaw, T. Mimura, B. F. Haynes, and J. B. Winfield.** 1990. Constitutive expression of a groEL-related protein on the surface of human γ/δ cells. J. Exp. Med. **172:**1857–1860.
25. **Jett, M., T. M. Seed, and G. A. Jamieson.** 1977. Isolation and characterization of plasma membranes and intact nuclei from lymphoid cells. J. Biol. Chem. **252:**2134–2142.
26. **Jones, D. B., A. F. W. Coulson, and G. W. Duff.** 1993. Sequence homologies between hsp60 and autoantigens. Immunol. Today **14:**115–118.
27. **Kaufmann, S. H. E.** 1991. Heat-shock proteins and pathogenesis of bacterial infections. Springer Semin. Immunopathol. **13:**25–36.
28. **Kaufmann, S. H. E.** 1990. Heat-shock proteins and the immune response. Immunol. Today. **11:**129–136.
29. **Khan, I. U., R. Wallin, R. S. Gupta, and G. M. Kammer.** 1998. Protein kinase A-catalyzed phosphorylation of heat shock protein 60 chaperone regulates its attachment to histone 2B in the T lymphocyte plasma membrane. Proc. Natl. Acad. Sci. USA **95:**10425–10430.
30. **Mayhew, M., A. C. R. da Silva, J. Martin, H. Erdjument-Bromage, P. Tempst, and F. U. Hartl.** 1996. Protein folding in the central cavity of the GroEL-GroES chaperonin complex. Nature **379:**420–426.
31. **McVay, L. D., B. Li, R. Biancaniello, M. A. Creighton, D. Bachwich, G. Lichtenstein, J. Rombeau, and S. R. Carding.** 1997. Changes in human mucosal γδ T cell repertoire and function associated with the disease process in inflammatory bowel disease. Mol. Med. **3:**183–203.
32. **Morimoto, R. I.** 1991. Heat shock: the role of transient inducible responses in cell damage, transformation and differentiation. Cancer Cells **3:**297–301.
33. **Morimoto, R. I., A. Tissières, and C. Georgopoulos.** 1989. Introduction to stress proteins, p. 1–30. *In* R. I. Morimoto and A. Tissières (ed.), The role of heat shock and stress response in biology and human disease. Cold Spring Harbor Laboratory Press, Cold Spring Harbor, N.Y.
34. **O'Brien, R. L., Y.-X. Fu, R. Cranfill, A. Dallas, C. Ellis, C. Reardon, J. Lang, S. R. Carding, R. Kubo, and W. Born.** 1992. heat shock protein Hsp60-reactive γδ cells; a large, diversified T-lymphocyte subset with highly focused specificity. Proc. Natl. Acad. Sci. USA **89:**4348–4352.
35. **O'Brien, R. L., M. P. Happ, A. Dallas, R. Cranfill, L. Hall, J. Lang, Y.-X. Fu, R. Kubo, and W. Born.** 1991. Recognition of a single hsp-60 epitope by an entire subset of γδ T lymphocytes. Immunol. Rev. **121:**155–169.

36. **Ozols, J.** 1990. Preparation of membrane fractions. Methods Enzymol. **182:** 225–235.
36a. **Nosheny, R., P. Egan, and S. R. Carding.** Unpublished observations.
37. **Peetermans, W. E., G. R. D'Haens, J. L. Ceuppens, P. Rutgeerts, and K. Geboes.** 1995. Mucosal expression by B7-positive cells of the 60-kilodalton heat-shock protein in inflammatory bowel disease. Gastroenterology **108:**75–82.
38. **Perraut, R., A. R. Lussow, S. Gavoille, O. Garraud, H. Matile, C. Tougne, J. van Embden, R. van der Zee, P.-H. Lambert, J. Gysin, and G. Del Giudice.** 1993. Successful primate immunization with peptides conjugated to purified protein derivative or mycobacterial heat shock proteins in the absence of adjuvants. Clin. Exp. Immunol. **93:**382–386.
39. **Peterman, G. M., C. Spencer, A. I. Sperling, and J. A. Bluestone.** 1993. Role of γδ T cells in murine collagen-induced arthritis. J. Immunol. **151:**6546–6558.
40. **Poccia, F., P. Piselli, S. Vendetti, S. Bach, A. Amendola, R. Placido, and V. Colizzi.** 1996. Heat-shock protein expression on the membrane of T cells undergoing apoptosis. Immunology **88:**6–12.
41. **Portnoy, D. A., R. K. Tweten, M. Kehoe, and J. Bielecki.** 1992. Capacity of listeriolysin O, streptolysin O, and perfringolysin O to mediate growth of *Bacillus subtilis* within mammalian cells. Infect. Immun. **60:**2710–2717.
42. **Roark, C. E., M. K. Vollmer, R. L. Cranfill, S. R. Carding, W. K. Born, and R. L. O'Brien.** 1993. Liver γδ T cells: TCR junctions reveal differences in heat shock protein-60-reactive cells in liver and spleen. J. Immunol. **150:** 4867–4875.
43. **Roseman, A. M., S. Chen, H. White, K. Braig, and H. R. Saibil.** 1996. The chaperonin ATPase cycle: mechanism of allosteric switching and movements of substrate-binding domains in GroEL. Cell **87:**241–251.
44. **Selmaj, K., C. F. Brosnan, and C. S. Raine.** 1991. Colocalization of lymphocytes bearing γδ T-cell receptor and heat shock protein hsp65$^+$ oligodendrocytes in multiple sclerosis. Proc. Natl. Acad. Sci. USA **88:**6452–6456.
45. **Selmaj, K., C. F. Brosnan, and C. S. Raine.** 1992. Expression of heat shock protein-65 by oligodendricytes *in vivo* and *in vitro*: implications for multiple sclerosis. Neurology **42:**795–802.
46. **Storrie, B., and E. A. Madden.** 1990. Isolation of subcellular organelles. Methods Enzymol. **182:**203–225.
47. **van Eden, W., J. E. R. Thole, R. van der Zee, A. Noordzij, J. D. A. van Embden, J. J. Henson, and I. R. Cohen.** 1988. Cloning of the mycobacterial epitope recognized by T lymphocytes in adjuvant arthritis. Nature **331:**171–173.
48. **Viitanen, P. V., A. A. Gatenby, and G. H. Lorimer.** 1992. Purified chaperonin 60 (groEL) interacts with the nonnative states of a multitude of *Escherichia coli* proteins. Protein Sci. **1:**363–369.
49. **Vincent, M. S., K. Roessner, D. Lynch, D. Wilson, S. M. Cooper, J. Tschopp, L. H. Sigal, and R. C. Budd.** 1996. Apoptosis of Fas-high CD4$^+$ synovial T ells by Borrelia-reactive Fas-ligand-high γδ T cells in Lyme arthritis. J. Exp. Med. **184:**2109–2117.

Editor: S. H. E. Kaufmann